

A Multi-Sensor Exportable Approach for Automatic Flooded Areas Detection and Monitoring by a Composite Satellite Constellation

Mariapia Faruolo, Irina Coviello, Teodosio Lacava, *Member, IEEE*, Nicola Pergola, and Valerio Tramutoli

Abstract—Timely and frequently updated information about flood-affected areas and their space-time evolution are often crucial in order to correctly manage the emergency phases. In such a context, optical data provided by meteorological satellites, offering the highest available temporal resolution (from hours to minutes), could have a great potential. As cloud cover often occurs reducing the number of usable optical satellite images, an appropriate integration of observations coming from different satellite systems will surely improve the probability to find cloud-free images over the investigated region. To make this integration effective, appropriate satellite data analysis methodologies, suitable for providing congruent results, regardless of the used sensor, are envisaged. In this paper, a sensor-independent approach (RST, Robust Satellites Techniques-FLOOD) is presented and applied to data acquired by two different satellite systems (Advanced Very High Resolution Radiometer (AVHRR) onboard National Oceanic and Atmospheric Administration platforms and Moderate Resolution Imaging Spectroradiometer (MODIS) onboard Earth Observing System satellites) at different spatial resolutions (from 1 km to 250 m) in the case of Elbe flood event occurred in Germany on August 2002. Results achieved demonstrated as the full integration of AVHRR and MODIS RST-FLOOD products allowed us to double the number of satellite passes daily available, improving continuity of monitoring over flood-affected regions. In addition, the application of RST-FLOOD to higher spatial resolution MODIS (250 m) data revealed to be crucial not only for mapping purposes but also for improving RST-FLOOD capability in identifying flooded areas not previously detected at lower spatial resolution.

Index Terms—AVHRR, Elbe river 2002 flood, MODIS, optical satellite sensors, RST-FLOOD.

I. INTRODUCTION

FLOODING is considered the most costly type of natural disaster, both in terms of damages and human casualties [25]. Satellite remote sensing technology is particularly employed today for supporting management and monitoring of flood situations [24], because it is able to furnish repetitive information, at various spatial and temporal resolutions, about location, extent, and dynamic evolution of the flooding event.

Manuscript received February 28, 2012; revised October 1, 2012; accepted December 2, 2012. Date of publication February 12, 2013; date of current version March 21, 2013.

M. Faruolo, I. Coviello, T. Lacava, and N. Pergola are with the Institute of Methodologies for Environmental Analysis, CNR, 85050 Tito Scalo (PZ), Italy (e-mail: mariapia.faruolo@imaa.cnr.it; irina.coviello@imaa.cnr.it; teodosio.lacava@imaa.cnr.it; nicola.pergola@imaa.cnr.it).

V. Tramutoli is with the University of Basilicata, 85100 Potenza, Italy (e-mail: valerio.tramutoli@unibas.it).

Color versions of one or more of the figures in this paper are available online at <http://ieeexplore.ieee.org>.

Digital Object Identifier 10.1109/TGRS.2012.2236336

It represents an economically viable alternative/complement to the traditional ground-based observation systems, often limited in terms of spatial distribution, temporal sampling and timeliness of data collection and transmission, [37]. The possibility to efficiently monitor floods during the crisis and early post-crisis phases is very important for supporting activities aimed at managing flood risk, helping in better assessing (and possibly mitigating) the impact in terms of human safety and infrastructure protection. This can be done with high temporal resolution sensors on board Earth Observation satellites, which can guarantee a steady and frequent stream of images for a timely and continuous investigation of environmental changes [1].

Synthetic aperture radar (SAR) systems, operating in the microwave region, in all illumination and weather conditions [24], have a great potential for flood mapping, thanks to the high sensitivity to the water presence as well as to a spatial resolution up to 1 m [25]. Also, high and very high spatial resolution optical sensors, on board LANDSAT, Satellite Pour l'Observation de la Terre (SPOT), Indian Remote Sensing (IRS), IKONOS, Earth Resources Observing System, and QuickBird, are able to provide, but only in absence of clouds, detailed information about Earth's surface, with a level of accuracy varying from tens of meters to tens of centimeters. Unfortunately such technologies present some issues and drawbacks when timely detection and continuous monitoring of space-time evolution of floods is aimed at, due to their poor temporal resolution (from weeks to some days) [6].

By the other side, optical instruments aboard polar and geostationary meteorological satellites, despite a coarse spatial resolution (from a few kilometers up to a few hundreds of meters), offer the highest temporal resolutions (from few hours up to 15 min) suitable for guaranteeing timely and frequently updated situation reports. The main limitation of such systems, apart from the medium-low spatial resolution, is that cloud presence can mask completely the surface, preventing any possibility to monitor phenomena occurring over it. Using very high temporal resolution systems or constellation of satellites carrying onboard similar sensors may help to overcome such an issue. Thanks to a suitable tradeoff among their high frequency, global coverage, multi-year operational continuity, full, and free availability of data [24], Advanced Very High Resolution Radiometer (AVHRR) and, more recently, Moderate Resolution Imaging Spectroradiometer (MODIS) data are widely used for flooded areas monitoring and mapping. AVHRR, in fact, can

assure imagery with a revisiting time less than 6 h and a spatial resolution of about 1100 m, while MODIS provides information up to 250 m of spatial resolution with a sampling frequency up to 3 h.

AVHRR [4], [8], [9], [17], [19], [21], [31], [34], [35], [48] and MODIS-based [2], [5], [18], [22], [23], [30], [38], [43], [49]–[51], [54] methods for flood detection and monitoring exploit the peculiar water behavior in the electromagnetic spectrum wavelength range between 0.4 μm and 1.7 μm . The common characteristic of such techniques is that they operate on the image at hand by applying threshold tests to different spectral indices (i.e., NDVI, NDWI, LSWI, EVI, etc.) which are implemented in decision tree-based chains to delineate water surface areas (e.g., [20], [36]).

In order to overcome major drawbacks of traditional single-image, fixed-threshold techniques, [20] applied a general multi-temporal change detection scheme named Robust AVHRR Technique [40], (now Robust Satellite Techniques, (RST) [41], [42]) to the detection and monitoring of flooded areas.

In this paper, the RST approach, here christened RST-FLOOD, has been implemented, for the first time, on MODIS 1 km data, to verify its exportability and, by comparison with results achievable with AVHRR, its actual sensor independence. To this aim, RST was applied to the same AVHRR bands [i.e., Visible (VIS) and Near Infrared (NIR)] of the previous study [20], even if, being sensor/signal independent, it can be easily applied to whatever index proposed in literature (i.e., NDVI, NDWI, LSWI, etc.) for detecting flooded areas.

In particular, advantages coming from an integrated (AVHRR+MODIS) multi-sensor system for a more effective flood detection and monitoring will be discussed. The same approach has been implemented on MODIS VIS and NIR channels at native spatial resolution (250 m) as well, to verify its increased performance not only for mapping but also for detection purposes.

Results and outcomes of these analyses will be shown and discussed in the case of the extreme flood event of the Elbe river that occurred on August 2002 in Germany.

II. THE RST METHODOLOGY AND RST-FLOOD PRODUCTS

The RST approach [41], [42] is a multi-temporal scheme of data analysis which identifies significant statistically anomalies of the investigated signal $V(x, y, t)$ [measured at time t for each pixel (x, y)] on the basis of a preliminary characterization of the signal in normal (i.e., unperturbed) conditions.

To this aim, a multi-year data-set of co-located imagery, collected around the same time of day during the same calendar month of the year of the image under investigation, is created to characterize the signal behavior, for each place (x, y) and time of observation t , in terms of expected value $\mu_V(x, y)$ and natural variability $\sigma_V(x, y)$. $\mu_V(x, y)$ and $\sigma_V(x, y)$ represent, respectively, the monthly temporal mean and the standard deviation of the signal under investigation; they are computed, for each pixel of the scene, processing all cloud-free records [41]. Cloudy pixels are identified applying the cloud detection scheme described in [7].

Signal anomalies are automatically identified in the space-time domain by the Absolutely Local Index of Change of the Environment (ALICE) index, so defined:

$$\otimes_V(x, y, t) = \frac{V(x, y, t) - \mu_V(x, y)}{\sigma_V(x, y)}$$

which provides, at pixel level, a measure of the deviation of the recorded signal $V(x, y, t)$ from its expected (in unperturbed or normal conditions) value (μ_V) and automatically compares this deviation with its normal variability (σ_V), which includes all the possible noise sources not related to the event to be monitored. The signal $V(x, y, t)$ is defined according to the type of phenomenon to be studied and may correspond to the measurement made in a single specific spectral band or derive from the combination of several channels [40]. No ancillary information about land cover and/or land use classes are required by such a not parametric approach. In fact, land spectral signatures mostly depend on vegetation cover and its seasonal variability which are completely taken into account by RST analysis: signals coming from each geographic location (co-located image pixel) are considered always in the same period of the year (i.e., the same month of the year when vegetation cover is expected to be about the same for the same location) about at the same time of the day, so ALICE index is expected to be completely independent not only on land cover but also on other site (e.g., orography) effects.

In this paper, following the previous and first application of RST in the flood risk assessment [20], the ratio and difference between VIS and NIR bands were used to discriminate flooded pixels.

In the VNIR (VIS+NIR) region of the electromagnetic spectrum, water exhibits a peculiar spectral behavior which is exploited to detect inundated areas. Compared to other common land covers and features (like bare or vegetated soils), in fact, water generally shows a reflectance in the NIR lower than in the VIS region. Therefore, in presence of water bodies or flooded areas, values lower than surroundings have to be expected for combinations of the spectral reflectances, R , acquired at these two wavelengths, like the ratio $R_{\text{NIR}}/R_{\text{VIS}}$ [33], [34] or the difference $R_{\text{NIR}} - R_{\text{VIS}}$ [48].

Hence, assuming $V(x, y, t)$ equal to the ratio $R_{\text{NIR}}/R_{\text{VIS}}$ [33], [34] and the difference $R_{\text{NIR}} - R_{\text{VIS}}$ [48] between reflectances, flooded areas were detected by the two following ALICE indices, representing two independent RST-FLOOD products, $\otimes_{\text{NIR-VIS}}(x, y, t) \equiv \text{ALICE}_{\text{NIR-VIS}}$ and $\otimes_{\text{NIR/VIS}}(x, y, t) \equiv \text{ALICE}_{\text{NIR/VIS}}$ [20]:

$$\begin{aligned} \otimes_{\text{NIR-VIS}}(x, y, t) &= \frac{R_{\text{NIR-VIS}}(x, y, t) - \mu_{\text{NIR-VIS}}(x, y)}{\sigma_{\text{NIR-VIS}}(x, y)} \end{aligned} \quad (1)$$

$$\begin{aligned} \otimes_{\text{NIR/VIS}}(x, y, t) &= \frac{R_{\text{NIR/VIS}}(x, y, t) - \mu_{\text{NIR/VIS}}(x, y)}{\sigma_{\text{NIR/VIS}}(x, y)}. \end{aligned} \quad (2)$$

In correspondence of flooded areas, negative $\otimes_{\text{NIR-VIS}}(x, y, t)$ (and $\otimes_{\text{NIR/VIS}}(x, y, t)$) values should be observed.

It should be noted that, differently from traditional fixed threshold methods, only newly flood-affected areas will be detected by RST-FLOOD, as signal (i.e., $R_{\text{NIR-VIS}}(x, y, t)$ or $R_{\text{NIR/VIS}}(x, y, t)$) measured in correspondence of permanent water bodies will exhibit no significant changes (i.e., $\otimes_{\text{NIR-VIS}}(x, y, t)$ and $\otimes_{\text{NIR/VIS}}(x, y, t)$ around zero) in comparison with its normal (i.e., $\mu_{\text{NIR-VIS}}(x, y)$ or $\mu_{\text{NIR/VIS}}(x, y)$) value.¹

Reference [20] demonstrated that the $\text{ALICE}_{\text{NIR-VIS}}$ is more sensitive to water presence while the $\text{ALICE}_{\text{NIR/VIS}}$ is expected to be more suitable (lower rate of false alarms) for a reliable identification of flood-affected area, thanks to the minor dependence of NIR/VIS spectral signature on observation conditions (e.g., illumination) variability [33]–[35].

Moreover, for their construction, both ALICE indices are standardized variables that, as the number N of the records increases, tend toward a Gaussian like distribution. Under this hypothesis, values of $\otimes_{\text{NIR/VIS}}$ (or $\otimes_{\text{NIR-VIS}}$) < -2 can be associated to events quite rare (probability of occurrence less than 2.5%) and values of $\otimes_{\text{NIR/VIS}}$ (or $\otimes_{\text{NIR-VIS}}$) < -3 to very rare events (probability of occurrence less than 0.13%). Hence, statistically significant signal anomalies are expected for $\otimes_{\text{NIR/VIS}}$ (or $\otimes_{\text{NIR-VIS}}$) < -2 at least, with increasing level of confidence moving to the lowest ones (i.e., -3 , -4).

The RST-FLOOD indices were implemented both on AVHRR channel 1 (0.58–0.68 μm —VIS) and channel 2 (0.73–1.00 μm —NIR) and, for the first time, on MODIS data, using corresponding VIS (0.62–0.67 μm) and NIR (0.841–0.876 μm) bands. Regarding these channels, as mentioned above, data at both available spatial resolutions (1000 m and 250 m) have been used. It should be noted that MODIS channels 1 and 2 are much narrower than AVHRR ones and have no overlap each other over the vegetation transition band; moreover, MODIS channel 1 is more shifted toward NIR region than the AVHRR channel 1 [43], [44]. Independent studies demonstrated that the different Spectral Response Functions of MODIS channels with respect to AVHRR ones lead to a surface reflectance difference of about 5% in the VIS channel and 10% in NIR channel [43]. Taking into account these considerations, we expect to observe a different sensitivity to the water presence by the use of these two sensors.

III. TEST CASE: THE AUGUST 2002 FLOOD EVENT

In August 2002, a catastrophic flooding hit the Central Europe and, in particular, the cities along the Elbe river in Germany (Fig. 1). Heavy rainfalls, produced by an extra tropical system classified as the Genoa Cyclone Type Vb, affected the southern part of Germany from August 11 to 13, causing damage quantified in more than 10 billion Euro [29]. On August 17, the Elbe inundated the city of Dresden [29], [45], [46]; soon afterward, the peak of water passed through Torgau and Wittenberg, inundating the entire Elbe floodplain. On

¹It should be noted that, like in the case of permanent water bodies, also areas which are systematically flooded during a particular period (month) of the year will be not detected as flooded by RST, which simply identifies anomalies in land surface conditions with reference to the site history at monthly temporal scale.

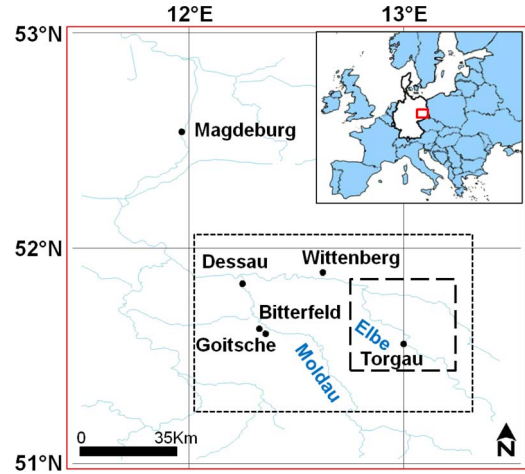


Fig. 1. Localization of the investigated area. In the red box, the portion of the Elbe river in Germany, hardly hit by the flood and analyzed by RST-FLOOD, is shown. Rivers have been depicted in blue, while the most flood-affected cities are marked with black dots. The areas within the dashed boxes have been used for AVHRR and MODIS results analyses (see text).

August 19 and 20, the runoff from the intense rainfall near the Czech-German border entered the Mulde river, which flooded downstream of the confluence with the Elbe, inundating the town of Bitterfeld [39], [45], [46]. The Mulde converged also on the Elbe, which inundated its floodplain upstream of Dessau [29]. Around 30% to 50% of the towns of Torgau, Wittenberg [45], [46], Dessau and Bitterfeld were submerged [29]. The Elbe river flood reached a width of 12 km and affected settlements as well as agricultural areas [55]. In particular, in the area of Bitterfeld, the intensity of flooding caused a break through of the Mulde river into the former lignite mining area of Goitsche [16]. The flood wave passed this area on August 24 [39].

In this paper, the Elbe river between Magdeburg and Torgau, about 450 km of length, along which the most inundated and damaged cities are dislocated, and the Mulde valley near Bitterfeld (Fig. 1) were particularly investigated.

IV. RST-FLOOD IMPLEMENTATION

Following the RST prescriptions, described in Section II, all reference fields ($\mu_{\text{NIR-VIS}}(x, y)$, $\mu_{\text{NIR/VIS}}(x, y)$, $\sigma_{\text{NIR-VIS}}(x, y)$, and $\sigma_{\text{NIR/VIS}}(x, y)$) were generated, at pixel level, for the investigated area shown in Fig. 1, by processing all MODIS diurnal passes (both at 1 km and 250 m of spatial resolution) collected between 8:30 and 13:00 GMT, in the month of August, between 2000 and 2007 (i.e., August 2001, August 2002, ... August 2007), excluding from computation the year of the flood (i.e., 7 years data-set) (327 images). All MODIS records identified as affected by clouds by the RST-based OCA cloud detection scheme (One-channel Cloudy radiance detection Approach, [7], with a $2 - \sigma$ cut for both visible and thermal radiances), have been excluded and not longer used for reference fields computation. For MODIS data at 250 m, the OCA has been implemented using only the visible radiances (channel 1). A similar procedure has been used for AVHRR. 185 images, acquired between 8:30 and 13:00 GMT, in the month of August, between 1998 and 2007 (i.e., 9 years

TABLE I
 AVHRR AND MODIS IMAGES USED FOR THE ANALYSES SHOWN IN THIS PAPER (MODIS IMAGES ARE HIGHLIGHTED IN THE GRAY BOX). COLUMN 3 REPORTS THE NUMBER OF ANOMALOUS PIXELS DETECTED WITHIN THE SMALLEST DASHED BOX SHOWN IN FIG. 1 FOR THE AVHRR-MODIS SEQUENCE

Acquisition date	Acquisition time (Satellite, Orbit number)	$\otimes_{NIR/VIS} <-2$	Cloud coverage (%)	Average sensor zenith angle (°)
August 16, 2002	10.45 GMT (TERRA, 14155)	28	0.30	33.3
	11.37 GMT (NOAA-16, 9790)	9	0.60	34.0
	13.16 GMT (NOAA-16, 9791)	2	0.80	59.7
August 17, 2002	9.50 GMT (TERRA, 14169)	14	0.58	39.7
	11.26 GMT (NOAA-16, 9804)	25	0.01	41.0
	13.05 GMT (NOAA-16, 9805)	15	0.30	53.0
August 18, 2002	11.15 GMT (NOAA-16, 9818)	2	0.16	44.7
	12.10 GMT (AQUA, 14185)	62	0.01	23.6
August 19, 2002	11.01 GMT (NOAA-16, 9831)	108	0.01	49.0
	11.15 GMT (AQUA, 14199)	182	0.00	46.3
	12.43 GMT (NOAA-16, 9833)	137	0.03	34.7
	12.55 GMT (AQUA, 14200)	124	0.02	61.1
August 20, 2002	10.20 GMT (TERRA, 14213)	200	0.00	0.8
	10.49 GMT (NOAA-16, 9832)	112	0.00	51.9
	12.00 GMT (AQUA, 14214)	194	0.00	6.1
	12.31 GMT (NOAA-16, 9847)	143	0.00	22.2
August 21, 2002	9.25 GMT (TERRA, 14227)	78	0.00	58.6
	11.05 GMT (AQUA, 14228)	115	0.00	54.8
	12.20 GMT (NOAA-16, 9861)	123	0.13	7.9
	12.40 GMT (AQUA, 14229)	74	0.36	53.6
August 22, 2002	10.05 GMT (TERRA, 14242)	76	0.38	17.4
	11.45 GMT (AQUA, 14243)	82	0.10	12.3
	12.09 GMT (NOAA-16, 9875)	54	0.07	7.5
August 23, 2002	10.50 GMT (TERRA, 14257)	35	0.00	39.6
	11.57 GMT (NOAA-16, 9889)	41	0.00	21.6

data-set, excluding 2002), were used for the analyses. Also, in this case, during the computation of the reference fields, cloudy records have been identified (and excluded) by applying the OCA scheme. In all cases, a buffer region of one pixel around the ones identified as cloudy by OCA was applied to prevent the presence of cloud shadows which, having a spectral behavior in the VNIR region similar to the one of flooded areas, may produce false alarms.

V. RESULTS

All the images reported in Table I were analyzed by using RST-FLOOD.

Results achieved by computing the $ALICE_{NIR/VIS}$ for the MODIS images at 1 km of spatial resolution are shown in Section V-A. Then, such results were compared to the ones obtained applying the same index on the AVHRR images (Section V-B) available in the analyzed period, to demonstrate their congruence as well as the added values achievable (thanks to such an intrinsic exportability) by their integration for timely and reliable identification of flooded areas. Section V-C is devoted to demonstrate the benefits coming from the use of $ALICE_{NIR-VIS}$ index (both for AVHRR and MODIS data) as far as a more detailed mapping of flooded areas (around the ones previously identified by $ALICE_{NIR/VIS}$) is concerned. Finally, the potential of higher spatial resolution RST-FLOOD product, achievable by using MODIS 250 m records, was investigated in Section V-D.

As far as validation is concerned, it should be emphasized that, with reference to the investigated region (Fig. 1), information available on flooded area refers mostly to urban zones

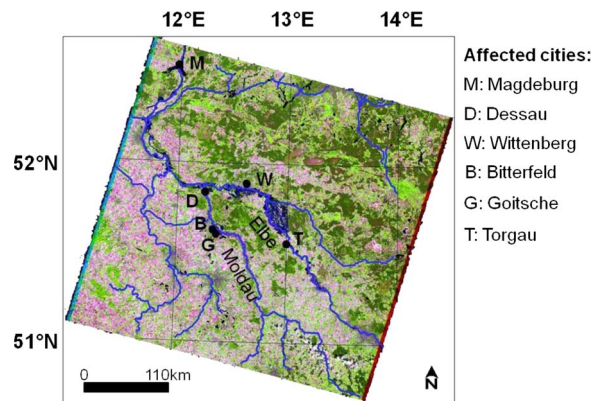


Fig. 2. RGB (543) of the LANDSAT-7 ETM+ image of August 20, 2002 (Path 193 and Row 24, with 30 m ground resolution), relative to the Elbe region. Rivers have been colored in blue, and the main affected cities are marked with black dots, while water-affected areas are highlighted in blue tones.

and punctual river level and discharge measurements, which scarcely help to validate large-scale products as the one generated by RST-FLOOD. This circumstance is quite usual and, by another point of view, this capability to provide large-scale 2-D maps, is also one of the main merits offered by satellite observations compared with traditional ones. However, "...on August 22, 2002, both the German Ministry of Interior and the Austrian Federal Warning Centre triggered the International Charter "Space and Major Disasters." This way, the satellite imagery provided by German Remote Sensing Data Center (DFD) and the Remote Sensing Technology Institute (IMF) and its partners ..." were used to integrate data provided by "...the European ERS-2, the Canadian RADARSAT, the French SPOT,

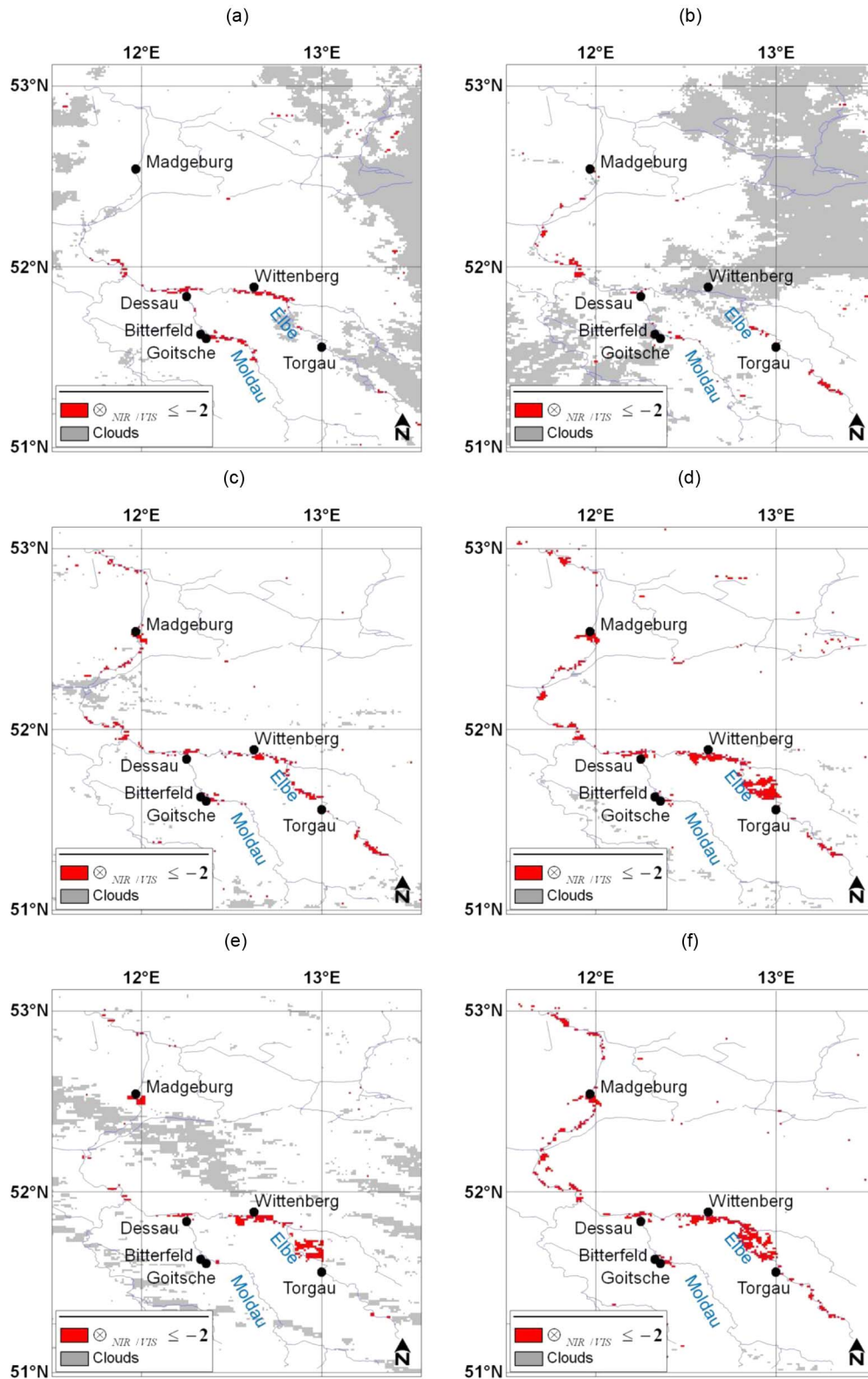


Fig. 3. Results obtained applying the $ALICE_{NIR/VIS} \leq -2$ (red pixels) to the MODIS images in the period August 16–23, 2002 are shown. Rivers have been depicted in blue and clouds in gray. The main affected cities are marked with black dots. (a) August 16, 2002—10.45 GMT; (b) August 16, 2002—09.50 GMT; (c) August 18, 2002—12.10 GMT; (d) August 19, 2002—11.15 GMT; (e) August 19, 2002—12.55 GMT; (f) August 20, 2002—10.20 GMT.

the Indian IRS and DLR's own BIRD satellite, making them available for situation assessment and crisis management . . .” [55]. All relevant high spatial resolution satellite data products available for the investigated area have been considered for

comparison, taking into account that spectral signatures of water bodies (and flooded areas) are quite strong both in the optical and SAR images. However, among the optical images available for the event (the complete list is reported by [16])

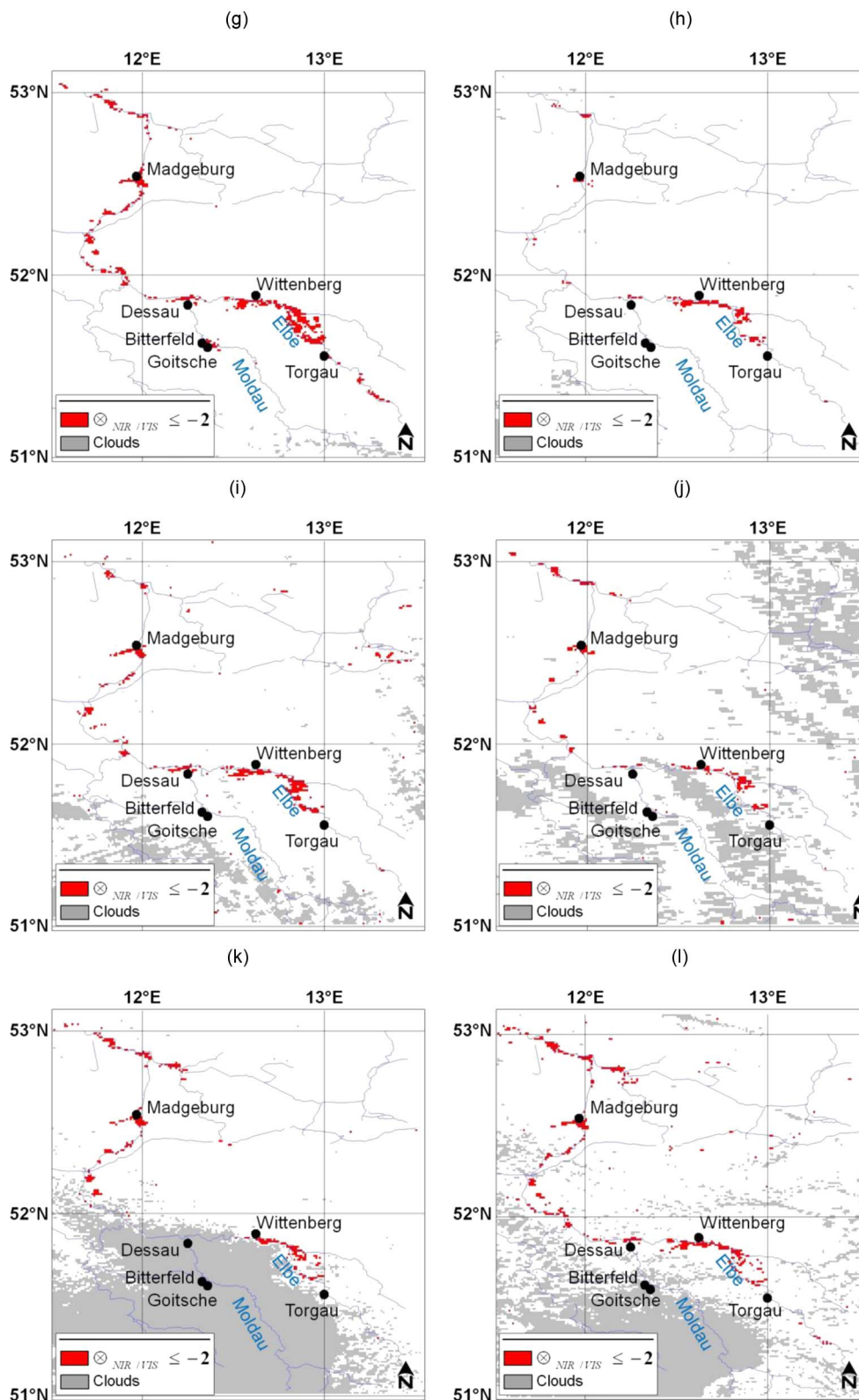


Fig. 3. (Continued.) Results obtained applying the $ALICE_{NIR/VIS} \leq -2$ (red pixels) to the MODIS images in the period August 16–23, 2002 are shown. Rivers have been depicted in blue and clouds in gray. The main affected cities are marked with black dots. (g) August 20, 2002—12.00 GMT; (h) August 21, 2002—09.25 GMT; (i) August 21, 2002—11.05 GMT; (j) August 21, 2002—12.40 GMT; (k) August 22, 2002—10.05 GMT; (l) August 22, 2002—11.45 GMT.

only one LANDSAT-7 ETM+ (WGS 84 UTM Zone 33S) image acquired on August 20, 2002 at 10.00 GMT [47] was usable to the scope (Fig. 2). Among the six SAR images [10] captured by ERS and Envisat satellites over the area affected by the Elbe

river flood (in support of requests from Switzerland, Austria, and Germany under the International Charter on Space and Major Disasters), only one product of the integration of SAR and optical data [12] was partly covering the area investigated

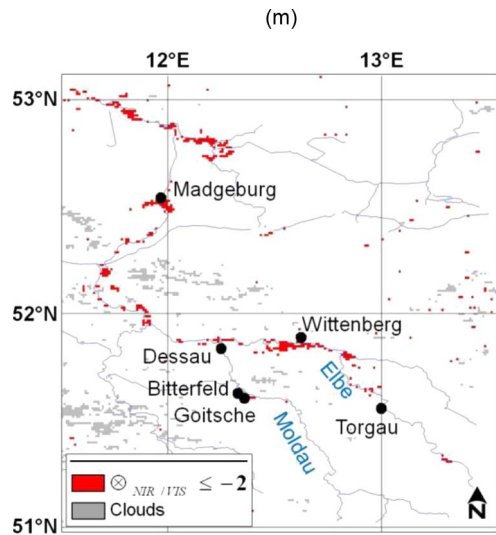


Fig. 3. (Continued.) Results obtained applying the $ALICE_{NIR/VIS} \leq -2$ (red pixels) to the MODIS images in the period August 16–23, 2002 are shown. Rivers have been depicted in blue and clouds in gray. The main affected cities are marked with black dots. (m) August 23, 2002—10.50 GMT.

in this paper. All these geospatial data, together with press release and local authorities reports, have been used as terms of reference for validating products presented in next sections.

A. Application to MODIS Radiances (1 km) for Floods Timely Detection and Monitoring

In this section, we move to assess RST-FLOOD exportability on MODIS data, at 1 km of spatial resolution. In Fig. 3, the results obtained applying the $ALICE_{NIR/VIS}$ to all the available MODIS images (Table I) are shown. In these pictures, only pixels (each representing an area of 1 km²) detected as anomalous ($\otimes_{NIR/VIS} < -2$) and/or cloud affected have been depicted over a white background.

Generally speaking, note that the anomalous pixels are mostly located along the river paths; hence, the hypothesis that such areas may be classified as flooded is more than realistic. In some images, a few anomalous pixels, which seem not related to flood, are present. If not to minor (not documented) flooded rivers, they may be associated to spurious effects due to illumination conditions as well as to residual cloud shadows effects, not correctly identified.

In detail, achieved results are in a generally good agreement with ground truth sources (according to, [3], [26], [29], [39]). In fact, space-time distribution of anomalies shown in Fig. 3 fully agrees with the description of the dynamics of the event independently given by [45], [46]. In particular, looking carefully at the temporal sequence, note that in the first available cloud-free image, dated August 16 at 10.45 GMT, some flooded pixels can be observed along the Elbe rivers [Fig. 3(a) and (b)], as a consequence of the rains felt until August 14. [26] reports that the peaks of water level were observed over the investigated area after August 18, when the Elbe received the contribution of the Mulde. According to such a report, a large number of flooded pixels were identified by $ALICE_{NIR/VIS}$ on August 19 and 20 [Fig. 3(d)–(g)], in the floodplain between Wittenberg

and Dessau [3], [11]–[13], [27], [32], [55], in the areas near Bitterfeld and at Magdeburg [14], [27]. After August 21 [Fig. 3(h)–(m)], in the floodplain between Wittenberg and Torgau and at Bitterfeld, it is possible to observe a slow return to normal conditions, except for the zone around Magdeburg, as confirmed by independent ERS observation reported by [52].

B. AVHRR and MODIS RST-FLOOD Products: Integration and Comparison

The full sequence of AVHRR and MODIS images available between August 16 and 23, 2002 is shown in Table I, containing also the number of pixels flagged as flood affected by $ALICE_{NIR/VIS}$ over the floodplain between Wittenberg and Torgau (the smallest dashed box in Fig. 1), one of the mostly affected zones. Moreover, the information about the average sensor zenith angle of images and the percentage of clouds within the box, which might help in the interpretation of results, are reported in such table.

A comparison between AVHRR and MODIS results was carried out considering among the available images the ones recorded very close in time (i.e., data acquired not more than 30 min apart) and having similar satellite zenith angle and cloud fraction, to minimize all the possible effects due to different observational conditions (e.g., relative sun position, atmospheric features, dynamics of flood). According to these criteria, the AVHRR and MODIS images of August 19 (acquired at 11.01 GMT and 11.15 GMT for AVHRR and MODIS, respectively), August 20 (acquired at 12.00 GMT and 12.31 GMT for MODIS and AVHRR, respectively), and the ones of August 22 (acquired at 11.45 GMT and 12.09 GMT for MODIS and AVHRR, respectively) were selected. Fig. 4 shows the pixels detected as flooded (red pixels) over the investigated area by implementing the $ALICE_{NIR/VIS}$ on AVHRR and MODIS data. Note, for the three considered days, the high correspondence between results, confirming the intrinsic exportability of RST-FLOOD, regardless the used sensor.

Table II summarizes the number of anomalies detected over the investigated area for these days: it is interesting to note the higher sensitivity of the $ALICE_{NIR/VIS}$ based on MODIS data for all days. As already mentioned, the relative surface reflectance difference between MODIS and AVHRR channels [43], [44], implying major values of NIR/VIS (and NIR-VIS) spectral signatures for MODIS, leads to a higher MODIS sensitivity than AVHRR, in the context of the RST approach.

Apart from these residual differences between MODIS and AVHRR-based systems, thanks to the high correspondence between results, RST-FLOOD can be seen as a multi-sensor exportable approach able to automatically detect flooded areas. The integration of the results achieved by such a multi-sensor configuration allows us to significantly increase the temporal frequency of obtained information. Such frequency, in fact, goes from 12 images per 8 days by using only AVHRR data (i.e., 1.5 images/day) to 25 images in the same period (about 3.0 images/day) integrating MODIS records, practically doubling the observational frequency. This gives the possibility to better follow the space-time evolution of flooded areas (updated information may be fundamental for the decision makers in

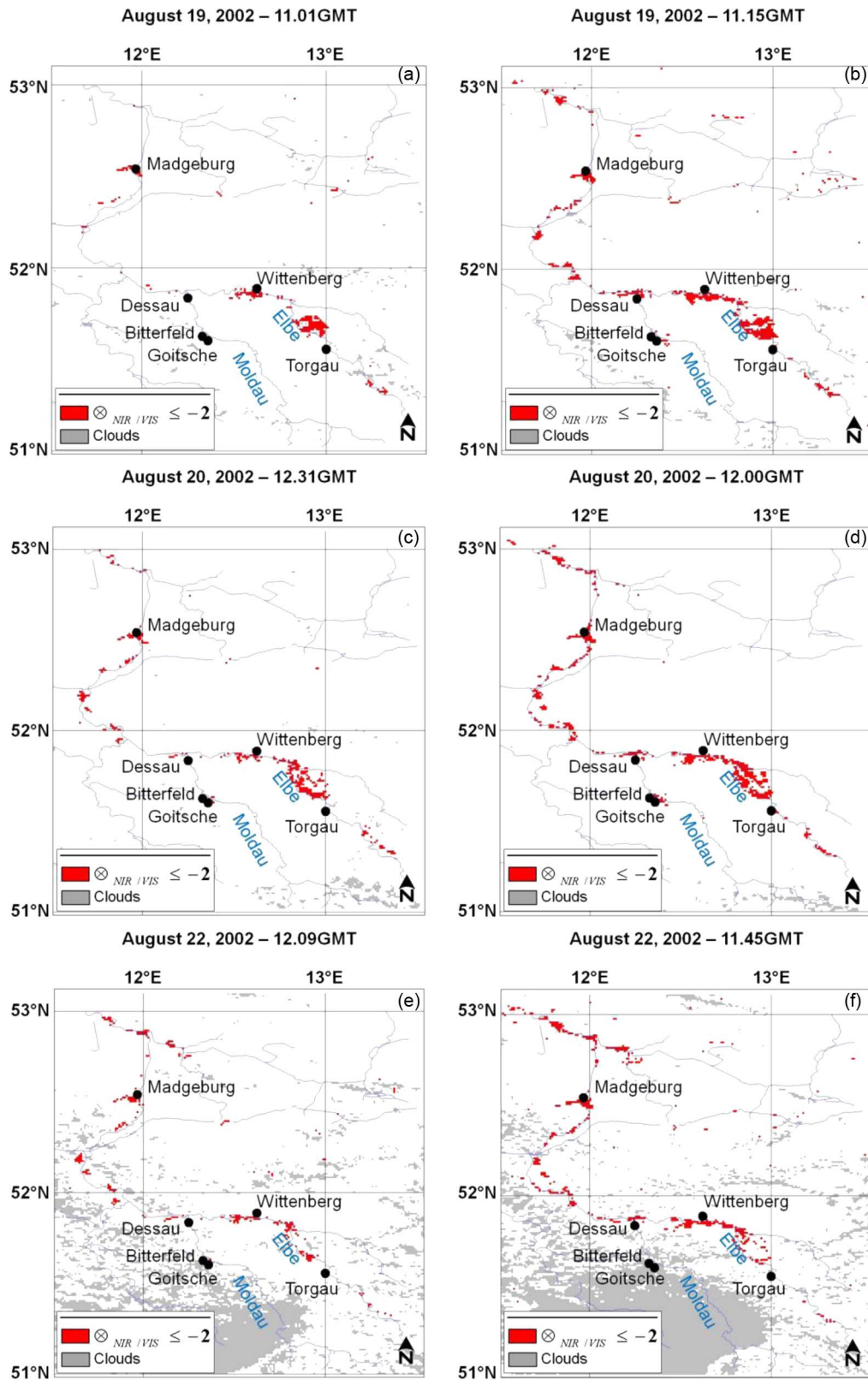


Fig. 4. Results obtained applying the $ALICE_{NIR/VIS} \leq -2$ (red pixels) to the AVHRR (a, c, e) and MODIS (b, d, f) images of August 19, 20, and 22, 2002 are shown. Rivers have been depicted in blue, and the main affected cities are marked with black dots.

order to better exploit their limited resources during the emergency phase) and also to reduce the impact of cloud cover (and/or of highly off-nadir images). A clear demonstration of this last point is observable in Fig. 5, where, on the left is depicted a

zoom over Wittenberg of the MODIS image of August 17, 2002 [Fig. 3(b)]. Because of the high clouds presence, no detection was possible for that image. The availability of the AVHRR passes, acquired at 11.26 GMT (Fig. 5, middle) and 13.05 GMT

TABLE II
NUMBER OF ANOMALOUS PIXELS DETECTED WITHIN THE INVESTIGATED AREA (FIG. 1) FOR THE AVHRR AND MODIS IMAGES OF AUGUST 19, 20, AND 22, BY IMPLEMENTING ALICE_{NIR/VIS}

Acquisition date	Acquisition time (GMT)	Sensor	$\otimes_{NIR/VIS} < -2$
August 19, 2002	11.01	AVHRR	288
	11.15	MODIS	553
August 20, 2002	12.00	MODIS	559
	12.31	AVHRR	338
August 22, 2002	11.45	MODIS	487
	12.09	AVHRR	280

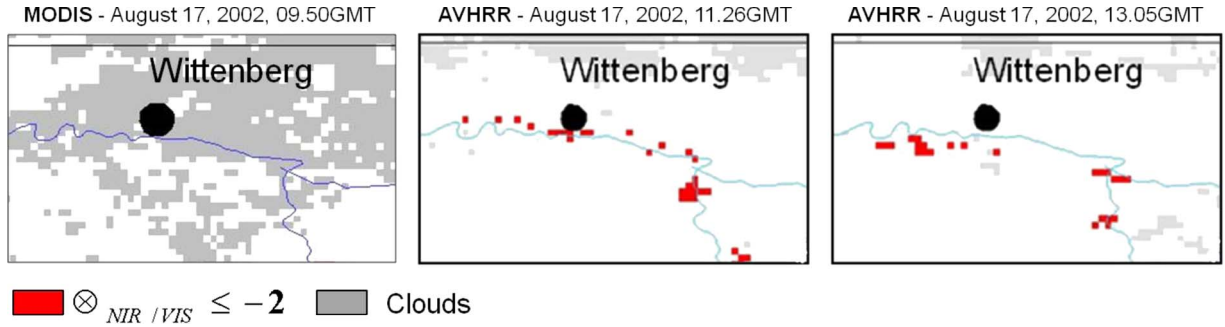


Fig. 5. On the left, a zoom of the MODIS image of August 17, 2002 at 9.50 GMT [Fig. 3(b)], cloudy around Wittenberg, at middle, and on the right, the cloud-free AVHRR passes for the same area and day (at 11.26 GMT and 13.05 GMT, respectively); in red, pixels detected as flooded applying the ALICE_{NIR/VIS} ≤ -2.

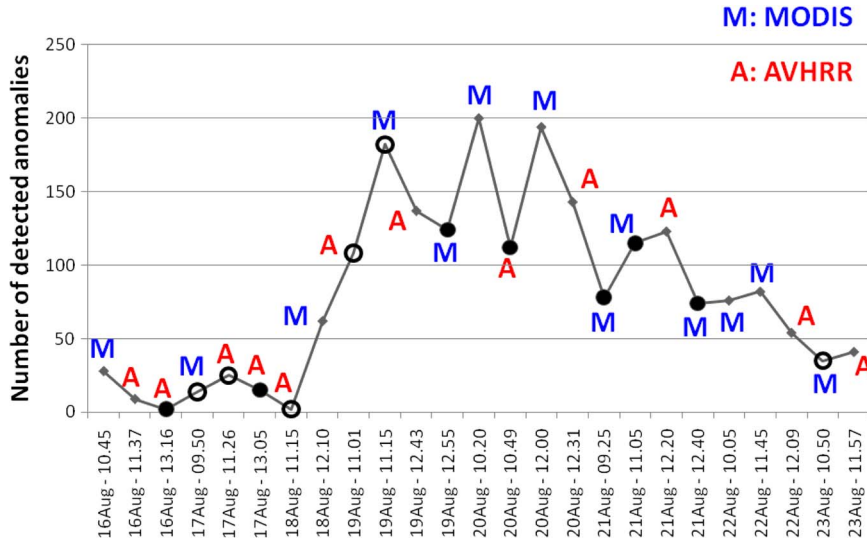


Fig. 6. Pixels detected as flooded applying the ALICE_{NIR/VIS} ≤ -2 to the AVHRR-MODIS sequence for the smallest dashed box shown in Fig. 1. Black empty dots are referred to images having a zenith angle between 35° and 50°, while the black filled ones zenith angles greater than 50°.

(Fig. 5, right), both cloud free over the above cited area, made it possible to overcome this gap and to identify the presence of wet soils (Fig. 5). As a demonstration of the potential of this integrated satellite system, Fig. 6 shows as the number of the detected flooded pixels allows us to follow the evolution of the flood dynamics in the considered period. Moreover, the integration of AVHRR and MODIS images allowed for a better evaluation of the extent of the areas involved in the flood. In Fig. 7, areas inundated by the Elbe flood, by exploiting the information coming from the integrated use of AVHRR and MODIS, are shown in red (e.g., 2248 pixels). It is evident as such an integration gives a clear benefit respect to the use of

one sensor. Only 1321 pixels (i.e., 59%) should have been in fact detected by AVHRR and 1711 (i.e., 76%) with MODIS.

C. Application to AVHRR and MODIS Radiances (1 km) for Floods Mapping

Fig. 2 shows an RGB combination (543) of the LANDSAT-7 ETM+ image acquired on August 20, 2002 at 10.00 GMT [47] used by different authors (e.g., [16], [55]) to identify (in blue tones on the picture) water-affected areas.

AVHRR and MODIS RST-FLOOD products obtained choosing the passes collected on August 20 as close as possible

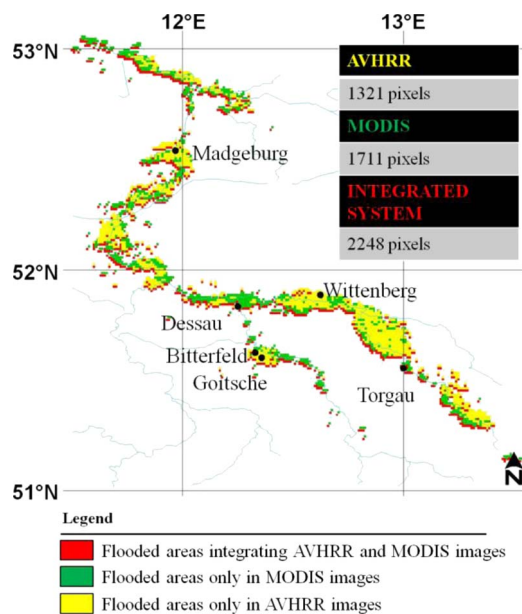


Fig. 7. Flood extent from August 16 to 23, 2002 by applying the $ALICE_{NIR/VIS} \leq -2$ on the AVHRR (yellow pixels), MODIS (green pixels), and both satellite images (red pixels).

(at 10.49 GMT and 10.20 GMT, respectively) to the time of LANDSAT-7 ETM+ image have been superimposed to this high spatial resolution image, to better evaluate the performance achievable by RST-FLOOD regarding to the precise mapping of flooded areas. To this aim, LANDSAT-7 ETM+ image was reprojected to AVHRR and MODIS spatial resolutions, identifying in such a way 875 pixels corresponding to the “water-affected areas,” then used as a reference for validating RST results. In such an analysis, both $ALICE_{NIR/VIS}$ and $ALICE_{NIR-VIS}$ indices have been computed, to enhance major differences and performances.

Looking at Fig. 8, it is possible to see as areas identified as flooded are in good spatial correlation with zones highlighted in LANDSAT-7 ETM+ RGB scene and well corresponding to all the other independent information available about the event [11], [12], [16], [27], [28], [55]. A quantitative analysis, consisting in the calculation of hits between pixels detected as flooded by RST indices and the water covered areas in the LANDSAT-7 ETM+, was performed; results are reported in Table III. Compared with water-affected areas highlighted by Fig. 2, it is possible to see that over 93% of pixels detected as flooded by both $ALICE_{NIR/VIS}$ and $ALICE_{NIR-VIS}$ implemented both on AVHRR and MODIS data (Table III) correspond to flooded areas identified by LANDSAT-7 ETM+. The very high agreement between the developed maps and the LANDSAT-7 ETM+ reference image confirms the high reliability of RST indices. The discrepancy between the 875 LANDSAT-7 ETM+ pixels and those detected as flooded by the $ALICE_{NIR-VIS}$ may be related to spurious effects due to illumination conditions as well as to residual cloud shadows effects, that if not correctly identified, may affect such an index.

Also, for this study case (as previously suggested by [20]) and for both sensors, $ALICE_{NIR/VIS}$ appears more protected than $ALICE_{NIR-VIS}$ against false alarms (due to particular

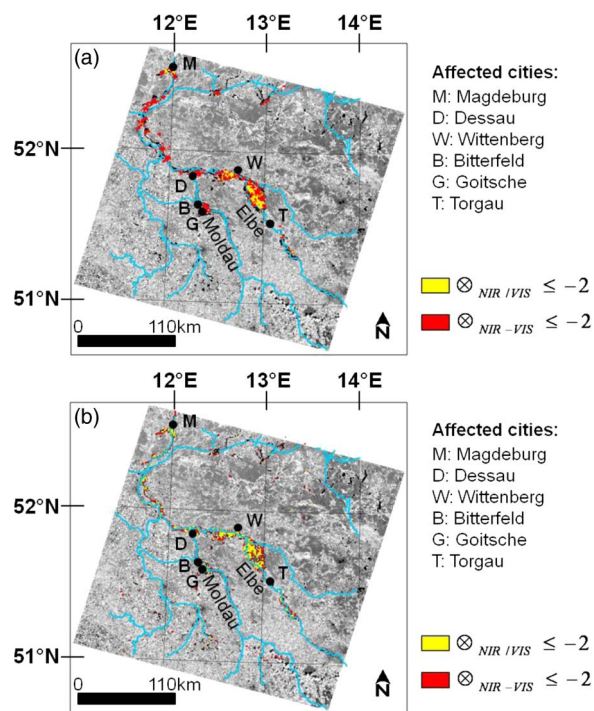


Fig. 8. Results obtained for the (a) AVHRR image of August 20, 2002 at 10.49 GMT and (b) MODIS image of August 20, 2002 at 10.20 GMT, by applying the $ALICE_{NIR-VIS}$ (red pixels) and $ALICE_{NIR/VIS}$ (yellow pixels), overlapped to the August 20, 2002 band 4 LANDSAT-7 ETM+ image. Rivers are reported in cyan, and the main affected cities are marked with black dots.

TABLE III
NUMBER OF PIXELS DETECTED AS FLOODED WITHIN THE LANDSAT-7 ETM+ SCENE (FIG. 2) FOR THE AVHRR AND MODIS IMAGES OF AUGUST 20 AT 10.49 GMT AND 10.20 GMT, RESPECTIVELY, BY IMPLEMENTING $ALICE_{NIR/VIS}$ AND $ALICE_{NIR-VIS}$ AND PERCENTAGE OF HITS RESPECT TO THE LANDSAT-7 ETM+ REFERENCE IMAGE

		AVHRR	MODIS
$ALICE_{NIR/VIS}$	Number of flooded pixels	197	517
	% of hits	96.4%	96.7%
$ALICE_{NIR-VIS}$	Number of flooded pixels	919	1044
	% of hits	93.5%	100%

illumination effects, cloud shadows, or features having a spectral signature similar to that of flooded areas), suggesting an operational strategy consisting in using the $ALICE_{NIR/VIS}$ to identify flooded areas with a high level of reliability (i.e., detection *for sure*, which might be done looking at the highest level of confidence of such a product) and the $ALICE_{NIR-VIS}$ for a more detailed description (i.e., mapping and monitoring) of affected areas around the pixels previously identified as flooded. As an example, we show the results achieved implementing such a strategy for the selected sub-scene (corresponding to the biggest dashed box in Fig. 1) of AVHRR and MODIS images on August 20, 2002, at 12.31 GMT and 12.00 GMT, respectively (Fig. 9). Observing such boxes, note as the $ALICE_{NIR/VIS}$ [Fig. 9(a)–(c)] detects a very few pixels but only (detection *for sure*) inside well-documented flooded areas [11], [12], [16], [27], [55], whereas with the $ALICE_{NIR-VIS}$, a better description of extent of flooded areas is possible [Fig. 9(b)–(d)] also at the same level of relative signal intensity.

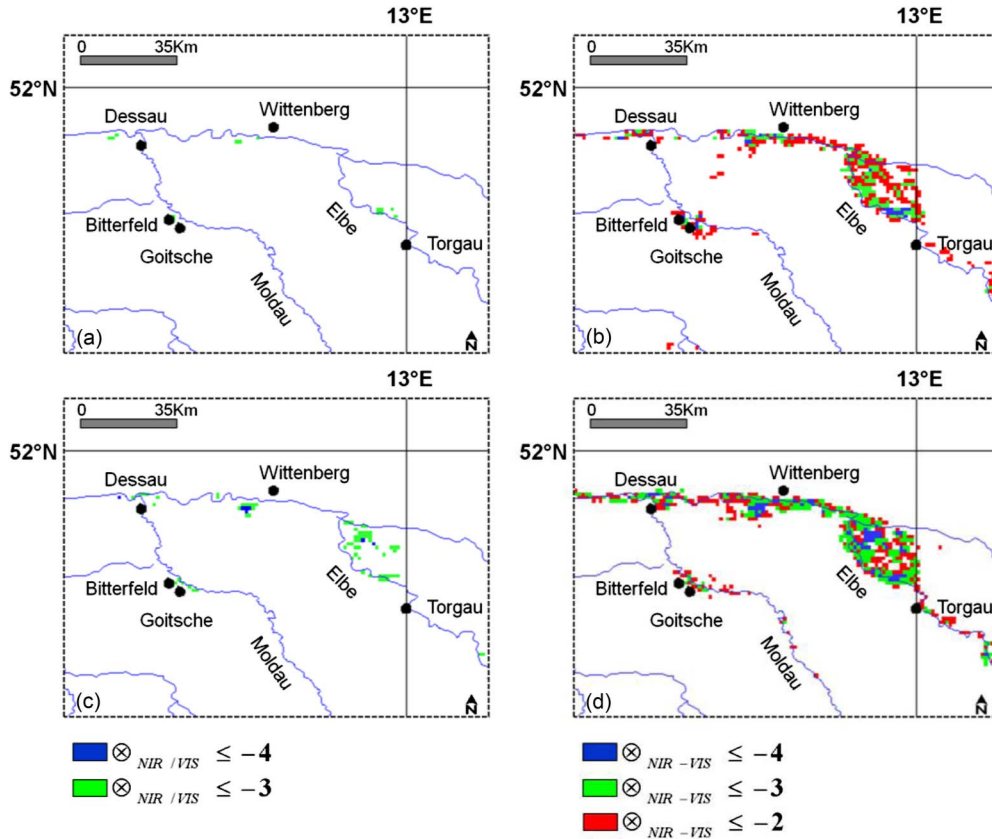


Fig. 9. Results obtained for the biggest dashed box in Fig. 1 for the AVHRR (a, b) and MODIS (c, d) images of August 20, 2002 (at 12.31 GMT and 12.00 GMT, respectively). (a)–(c) Pixels detected as flooded by the ALICE_{NIR/VIS} ($\otimes_{NIR/VIS} \le -3, \le -4$); (b)–(d) pixels detected as flooded by the ALICE_{NIR-VIS} ($\otimes_{NIR-VIS} \le -4, \le -3, \le -2$), depicted in different colors according to index intensity.

D. Application to MODIS Radiances (250 m) for Improving Flooded Areas Identification and Mapping

The last step of this work has regarded the implementation of the proposed approach on high-resolution (250 m) MODIS data to verify whether an improvement in mapping capability of flooded areas (as expected) might be actually obtained. Taking into account the results just achieved, the ALICE_{NIR-VIS} has been used to better highlight flooded areas.

In Fig. 10, a comparison between the results obtained by implementing the ALICE_{NIR-VIS}, at 1 km [Fig. 10(a)] and at 250 m [Fig. 10(b)], is shown. It refers to the analysis performed on the area within the biggest dashed box marked in Fig. 1 using the MODIS image acquired on August 21, at 9.25 GMT. Looking at the figure, the advantage of using a higher spatial resolution is quite evident. Already detected flood-affected areas are identified with a higher detail (see for instance the areas around Dessau and those between Wittenberg and Torgau). Moreover, new water-affected areas are detected as far as 250 m data are used (see the zones highlighted by the black arrows downstream of Torgau, to both sides of Dessau and that between Bitterfeld and Goitsche), showing as improving spatial resolution also results in enhancing sub-pixel detection capability (because water-affected pixel fraction increases as far as pixel size decreases). As a consequence, RST-FLOOD applied to 250 m MODIS data allows for an improved mapping of inundated areas, better describing the spatial extent of the event along the Elbe river, as well it is appreciable looking at

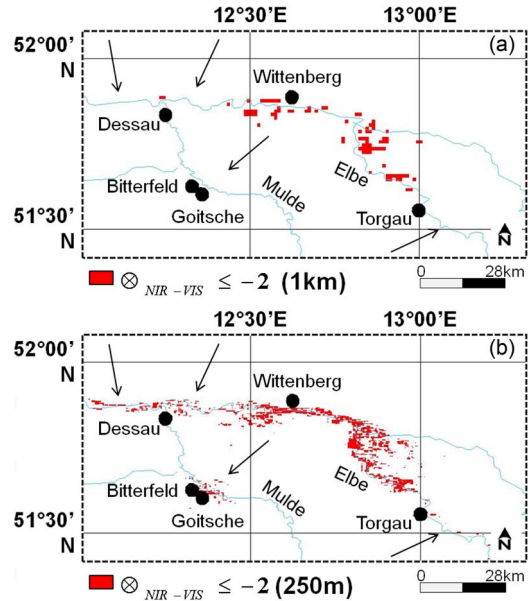


Fig. 10. Results obtained by applying the ALICE_{NIR-VIS} on the biggest dashed box shown in Fig. 1, relative to MODIS image of August 21 at 9.25 GMT, at (a) 1 km and (b) 250 m, respectively, are shown.

the Fig. 10(b), where flooded areas are enhanced, compared to the ones identified at 1000 m [Fig. 10(a)], with a major spatial continuity (e.g., between west of Dessau and south east of Torgau). To provide a quantitative evaluation of such an

improved mapping capability, an estimation of flood-affected areas (in terms of square kilometers) was performed for both spatial resolutions (1000 m and 250 m) within the region shown in Fig. 10 starting from ALICE_{NIR-VIS} products. About 88 km² of land were estimated as inundated by using data at 1000 m whereas as far as 250 m data were employed, the estimated flood area was more than doubled (i.e., 176 km²).

VI. CONCLUSION

In this paper, the intrinsic exportability of the proposed RST-FLOOD approach for flooded areas monitoring and mapping was fully assessed and demonstrated after its application on different satellite sensors (National Oceanic and Atmospheric Administration-AVHRR and Earth Observing System-MODIS) and at various spatial resolutions (MODIS at 1 km and 250 m channels), in the case of the Elbe river flood that occurred in Germany on August 2002.

The comparison between results obtained implementing such an approach on AVHRR and MODIS data showed its similar capability to correctly identify flooded areas and to properly follow event evolution in space-time domain, in accordance with independent information and relevant bulletins and reports.

For instance, the comparison with independently obtained (by LANDSAT-7 ETM+ data) flooded area maps revealed up to a 100% of correct identifications for MODIS (96% for AVHRR).

The high correspondence between AVHRR and MODIS-based results strengthened the added value of an integrated use of multi-sensors data for flooding event detection and monitoring. Combining AVHRR and MODIS images allowed an increase of the observational frequency of a factor 2 (passing from 1.5 to 3 images/day), significantly improving flood evolution monitoring. In addition, integrating multi-sensor data-sets will generally increase the probability of clear sky acquisitions, reducing the cloud problem, one of the main limitations of optical satellite observations, particularly for this kind of applications. Moreover, the integration of AVHRR and MODIS images allowed for a significant (up to 41%) increase of the extent of the flooded area identified by a single sensor. This could be particularly important for post-event damage assessment purposes as well as for drawing or updating flood risk maps.

Regardless of the used sensor, RST-FLOOD detects as flooded quite the same area extents, even if a major sensitivity of MODIS compared with AVHRR has been enhanced and interpreted on the base of the different spectral features of the two sensors. Furthermore, concerning differences between the RST-FLOOD indices (ALICE_{NIR-VIS} ALICE_{NIR/VIS}), achieved results confirmed, for both the used sensors, a major robustness (against possible false alarms) of the ALICE_{NIR/VIS}, to be used for a detection *for sure* of flooded pixels and a higher sensitivity of the ALICE_{NIR-VIS}, more suitable to accurately map water inundated areas. Finally, in this context, the use of MODIS data at 250 m is demonstrated to be useful, not only to improve mapping capabilities (flooded area size doubled when passing from 1000 m to 250 m MODIS data-set) but also for detection purposes, identifying water inundated areas of small extent that remained undetected by using 1000 m

data. Present RST-FLOOD limitations to daylight monitoring (due to the use of VNIR radiances) is expected to be overcome by its extension to thermal infrared (TIR) radiances. Preliminary encouraging results in this direction have been already achieved by [15], suggesting the possibility for an actual all day RST-FLOOD-based monitoring system. In such a system, VNIR data provided by the Visible Infrared Imaging Radiometer Suite (VIIRS) on board of Suomi-National Polar-orbiting Partnership will be also taken into account. VIIRS channels I1 (0.600–0.680 μm) and I2 (0.846–0.886 μm), in fact, present the same spectral features of MODIS channel 1 and 2, with an almost similar spatial resolution (375 m). In addition, VIIRS data are acquired at 13:30 LTAN, as AQUA ones. So that, until long-term historical series of VIIRS data will be not available, AQUA references fields can be re-sampled at VIIRS spatial resolution in order to apply the approach proposed in this work.

REFERENCES

- [1] M. S. Aduah, "Multitemporal Remote Sensing for Mapping and Monitoring Floods. An Approach Towards Validation of the KAFRIBA Model, Kafue Flats, Zambia," M.S. thesis, Geo-Information Science and Earth Observation for Environmental Modelling and Management, Univ. Southampton, Southampton, U.K., 2007.
- [2] E. Anderson, G. R. Brakenridge, and S. Caquard, Dartmouth Atlas of Global Flood Hazard: E100N20, Dartmouth Flood Observatory, Hanover, NH. [Online]. Available: <http://www.dartmouth.edu/~floods/hydrography/E100N20.html>
- [3] H. Bach, U. Dierschke, F. Appel, A. Fellah, and P. de Fraipont, "Application of satellite data for flood monitoring," in *Proc. IEEE IGGARS*, Göttingen, Germany, 2004, pp. 1–5.
- [4] I. J. Barton and J. M. Bathols, "Monitoring floods with AVHRR," *Remote Sens. Environ.*, vol. 30, no. 1, pp. 89–94, Oct. 1989.
- [5] G. R. Brakenridge, J. P. M. Syvitski, I. Overeem, J. A. Stewart-Moore, and A. J. Kettner, "Global mapping of storm surges, 2002-present and the assessment of coastal vulnerability," *Nat. Hazards*, 2012, to be published.
- [6] "The Use of Earth Observing Satellites for Hazard Support: Assessments and Scenarios—Final Report of the CEOS Disaster Management Support Group (DMSG)," Washington, DC, Nov. 2003.
- [7] V. Cuomo, C. Filizzola, N. Pergola, C. Pietrapertosa, and V. Tramutoli, "A self-sufficient approach for GERB cloudy radiance detection," *Atmos. Res.*, vol. 72, no. 1–4, pp. 39–56, Nov./Dec. 2004.
- [8] N. R. Dalezios, C. Domenikiotis, S. T. Tzortzios, and C. Kalaitzidis, "Cotton yield estimation based on NOAA/AVHRR produced NDVI," *Phys. Chem. Earth B, Hydrol., Oceans Atmos.*, vol. 26, no. 3, pp. 247–251, 2001.
- [9] C. Domenikiotis, A. Loukas, and N. R. Dalezios, "The use of NOAA/AVHRR satellite data for monitoring and assessment of forest fires and floods," *Nat. Hazards Earth Syst. Sci.*, vol. 3, no. 1/2, pp. 115–128, 2003.
- [10] ESA, 2002. [Online]. Available: http://www.esa.int/esaCP/ESAZODZPD4D_index_1.html#subhead1
- [11] ESA, (2005). [Online]. Available: http://www.esa.int/esaEO/SEMR8C6Y3EE_index_1.html
- [12] ESA, (2005). [Online]. Available: http://esamultimedia.esa.int/images/EarthObservation/PI_of_the_month/2005-08-16/Flood_Agriculture_H.jpg
- [13] EUROMAP, (2006, May 30). [Online]. Available: http://www.euromap.de/samples/exam_080.html
- [14] EUROMAP, (2006, May 30). [Online]. Available: http://www.euromap.de/samples/exam_115.html
- [15] M. Faruolo, I. Coviello, T. Lacava, N. Pergola, and V. Tramutoli, "On the potential of Robust Satellite Technique (RST) approach for flooded areas detection and monitoring using thermal infrared data," in *Proc. IEEE Int. Geosci. Remote Sens. Symp.*, 2010, pp. 914–917.
- [16] C. Gläßer and P. Reinartz, "Multitemporal and multispectral remote sensing approach for flood detection in the Elbe-Mulde Region 2002," *Acta Hydrochim. Hydrobiol.*, vol. 33, no. 5, pp. 395–403, Dec. 2005.
- [17] M. M. Islam and S. Kimiteru, "Flood hazard assessment in Bangladesh using NOAA AVHRR data with geographical information system," *Hydrol. Process.*, vol. 14, no. 3, pp. 605–620, Feb. 2000.

- [18] A. S. Islam, S. K. Bala, and M. A. Haque, "Flood inundation map of Bangladesh using MODIS time-series images," *J. Flood Risk Manage.*, vol. 3, no. 3, pp. 210–222, Sep. 2010.
- [19] S. K. Jain, A. K. Saraf, A. Goswami, and T. Ahmad, "Flood inundation mapping using NOAA AVHRR data," *Water Resources Manage.*, vol. 20, no. 6, pp. 949–959, Dec. 2006.
- [20] T. Lacava, N. Pergola, F. Sannazzaro, and V. Tramutoli, "Improving flood monitoring by the Robust AVHRR Technique (RAT) approach: The case of the April 2000 Hungarian flood," *Int. J. Remote Sens.*, vol. 31, no. 8, pp. 2043–2062, Apr. 2010.
- [21] C. Lin, "Applying meteorological satellite information to monitor water-logging in Heilongjiang Province," (in Chinese), *Remote Sens. Inf.*, no. 3, pp. 24–28, 1989.
- [22] J. Low, S. C. Liew, and L. K. Kwoh, "Automated near-real-time flood detection and mapping using Terra MODIS," in *Proc. 25th Asian Conf. Remote Sens.*, Chiang Mai, Thailand, Nov. 22–26, 2004, pp. 221–225.
- [23] J. Low, S. C. Liew, A. Lim, A. W. C. Heng, and L. K. Kwoh, "MODIS direct broadcast data for environmental monitoring in Southeast Asia," in *Proc. 2nd ASEAN Sci. Conf., Sub-Committee on Space Technol. Appl. (SCOSA)*, Jakarta, Indonesia, Aug. 5–6, 2005, pp. 1–4.
- [24] E. Malnes, S. Solbø, I. Lauknes, G. J. Evertsen, T. A. Tøllefsen, I. Solheim, and M. Indregard, "FloodMan-Global near real-time flood monitoring for hydrological users," in *Proc. ACTIF Workshop*, Tromsø, Norway, Oct. 17–19, 2005, pp. 1–9.
- [25] S. Martinis, A. Twele, and S. Voigt, "Towards operational near real-time flood detection using a split-based automatic thresholding procedure on high resolution TerraSAR-X data," *Nat. Hazards Earth Syst. Sci.*, vol. 9, no. 2, pp. 303–314, Mar. 2009.
- [26] M. Mudelsee, M. Börngen, G. Tetzlaff, and U. Grunewald, "Extreme floods in central Europe over the past 500 years: Role of cyclone pathway 'Zugstrasse Vb'," *J. Geophys. Res.*, vol. 109, no. D23, pp. D23101–1–D23101–21, Dec. 2004.
- [27] NASA. 2002. [Online]. Available: http://commons.wikimedia.org/wiki/File:NASA_Elbe_flood_2002_before_after.jpg
- [28] G. Petrie, "After the deluge: Flooding in middle europe observed from space," *GeoInformatics*, vol. 5, no. 7, pp. 6–9, Oct./Nov. 2002.
- [29] "Central Europe Flooding, August 2002," Newark, CA, Event Rep., 2003.
- [30] T. Sakamoto, N. V. Nguyen, A. Kotera, H. Ohno, N. Ishitsuka, and M. Yokozawa, "Detecting temporal changes in the extent of annual flooding within the Cambodia and the Vietnamese Mekong Delta from MODIS time-series imagery," *Remote Sens. Environ.*, vol. 109, no. 3, pp. 295–313, Aug. 2007.
- [31] J. Sanyal and X. X. Lu, "Application of remote sensing in flood management with special reference to monsoon Asia: A review," *Nat. Hazards*, vol. 33, no. 2, pp. 283–301, Oct. 2004.
- [32] Sciencephoto, 2002. [Online]. Available: <http://www.sciencephoto.com/media/164030/view>
- [33] Y. Sheng, Q. Xiao, and W. Chen, "Flood monitoring using FY-1B satellite data," (in Chinese), *Remote Sens. Environ. China*, vol. 9, no. 3, pp. 228–233, 1994.
- [34] Y. W. Sheng, Y. F. Su, and Q. G. Xiao, "Challenging the cloud-contamination problem in flood monitoring with NOAA/AVHRR imagery," *Photogramm. Eng. Remote Sens.*, vol. 64, no. 3, pp. 191–198, Mar. 1998.
- [35] Y. Sheng, P. Gong, and Q. Xiao, "Quantitative dynamic flood monitoring with NOAA AVHRR," *Int. J. Remote Sens.*, vol. 22, no. 9, pp. 1709–1724, Jun. 2001.
- [36] P. Song and Y. Liu, "Temporal influences on thresholding for satellite retrieval of water surface areas: A case in the Poyang Lake, China," in *Proc. 6th Int. Conf. WiCOM Netw. Mob. Comput.*, Chengdu, China, 2010, pp. 1–4.
- [37] G. Stancalie and V. Craciunescu, "Contribution of Earth Observation data supplied by the new satellite sensors to flood disaster assessment and hazard reduction," in *Geo-Information for Disaster Management*, P. van Zlatanova and E. M. Fendel, Eds. New York: Springer-Verlag, 2005, pp. 1315–1332.
- [38] D. L. Sun and Y. Y. Yu, "Deriving water fraction and flood map with the EOS/MODIS data using regression tree approach," in *Proc. ISPRS TC VII Symp.—100 Years*, W. Wagner and B. Székely, Eds., Vienna, Austria, Jul. 5–7, 2010, vol. 38, pp. 552–556.
- [39] J. Toothill, "Central European Flooding August 2002," ABS Consulting, Houston, TX, Tech. Rep. EQECAT, 2002.
- [40] V. Tramutoli, "Robust AVHRR Techniques (RAT) for Environmental Monitoring: Theory and applications," in *Proc. SPIE Earth Surface Remote Sens. II*, E. Zilioli, Ed., Giovanna Cecchi, 1998, vol. 3496, pp. 101–113.
- [41] V. Tramutoli, "Robust Satellite Techniques (RST) for natural and environmental hazards monitoring and mitigation: Ten years of successful applications," in *Proc. 9th ISPRS Phys. Meas. Sign. Remote Sens.*, S. Liang, J. Liu, X. N. Li, R. Liu, and M. Schaepman, Eds., Beijing, China, 2005, vol. 37, pp. 792–795.
- [42] V. Tramutoli, "Robust Satellite Techniques (RST) for natural and environmental hazards monitoring and mitigation: Theory and applications," in *Proc. 4th Int. Workshop Anal. MultiTemp. Remote Sens. Images*, Louven, Belgium, Jul. 18–20, 2007, pp. 1–6.
- [43] A. P. Trishchenko, J. Cihlar, and Z. Q. Li, "Effects of spectral response function on surface reflectance and NDVI measured with moderate resolution satellite sensors," *Remote Sens. Environ.*, vol. 81, no. 1, pp. 1–18, Jul. 2002.
- [44] A. P. Trishchenko, "Effects of spectral response function on surface reflectance and NDVI measured with moderate resolution satellite sensors: Extension to AVHRR NOAA-17, 18 and METOP-A," *Remote Sens. Environ.*, vol. 113, no. 2, pp. 335–341, Feb. 2009.
- [45] U. Ulbricht, T. BruÈcher, A. H. Fink, G. C. Leckebusch, A. KruÈger, and J. G. Pinto, "The central European floods of August 2002Part 1: Rainfall periods and flood development," *Weather*, vol. 58, no. 10, pp. 371–377, Oct. 2003.
- [46] U. Ulbricht, T. BruÈcher, A. H. Fink, G. C. Leckebusch, A. KruÈger, and J. G. Pinto, "The central European floods of August 2002Part 2: Synoptic causes and considerations with respect to climatic change," *Weather*, vol. 58, no. 11, pp. 434–442, Nov. 2003.
- [47] USGS, "NASA Landsat Program, Landsat ETM+ Scene L72193024_02420020820, L1G, USGS, 08/20/2002, Path 193, Row 24, Courtesy of the U.S. Geological Survey," Reston, VA, 2010. [Online]. Available: <http://landsat.usgs.gov>
- [48] Q. Xiao and W. Chen, "Songhua River flood monitoring with meteorological satellite imagery," (in Chinese), *Remote Sens. Inf.*, no. 4, pp. 37–41, 1987.
- [49] X. M. Xiao, S. Boles, J. Y. Liu, D. F. Zhuang, S. Frolking, C. S. Li, W. Salas, and B. Moore, "Mapping paddy rice agriculture in southern China using multi-temporal MODIS images," *Remote Sens. Environ.*, vol. 95, no. 4, pp. 480–492, Apr. 2005.
- [50] X. M. Xiao, S. Boles, S. Frolking, C. S. Li, J. Y. Babu, W. Salas, and B. Moore, "Mapping paddy rice agriculture in South and Southeast Asia using multi-temporal MODIS images," *Remote Sens. Environ.*, vol. 100, no. 1, pp. 95–113, Jan. 2006.
- [51] Y. E. Yan, Z. T. Ouyang, H. Q. Guo, S. S. Jin, and B. Zhao, "Detecting the spatiotemporal changes of tidal flood in the estuarine wetland by using MODIS time series data," *J. Hydrol.*, vol. 384, no. 1/2, pp. 156–163, Apr. 2010.
- [52] H. Yesou, "Methods and possibilities of spatial techniques in flood rapid mapping and flood risk management," in *Proc. Dragon Meeting*, Xiamen, China, Apr. 28th, 2004, pp. 1–21.
- [53] X. Zhan, R. A. Sohlberg, J. R. G. Townshend, C. DiMiceli, M. L. Caroll, J. C. Eastman, M. C. Hansen, and R. S. DeFries, "Detection of land cover change using MODIS 250 m data," *Remote Sens. Environ.*, vol. 83, no. 1/2, pp. 336–350, Nov. 2002.
- [54] N. Zheng, K. Takara, Y. Tachikawa, and O. Kozan, "Analysis of vulnerability to flood hazard based on land use and population distribution in the Huaihe River Basin, China," in *Proc. Annu. Disas. Prev. Res. Inst., Kyoto Univ.*, 2008, vol. 51B, pp. 83–90.
- [55] ZKI. 2002. [Online]. Available: <http://www.zki.dlr.de/article/1047>



Mariapia Faruolo was born in Potenza, Italy, in 1980. She received the Master's and Ph.D. degrees in environmental engineering from the University of Basilicata, Potenza, in 2006 and 2012, respectively.

Since 2007, she has been collaborating with the Institute of Methodologies for Environmental Analysis, National Research Council, Tito Scalo, Potenza. She is one of the researchers working for the Basilicata region Val d'Agri Environmental Observatory. Her main research activity is focused on the development of robust satellite techniques for near-

real-time detection and monitoring of flooded areas. In her study, she exploits data acquired both by optical and microwave sensors. She has been a Coinvestigator of several Italian Space Agency, CNR, and European Union projects. She is also the author of several peer-reviewed scientific journal articles.



Irina Coviello was born in Potenza, Italy, in 1982. She received the Master's degree in computer sciences from the University of Basilicata, Potenza, Italy, in 2006, where she is currently working toward the Ph.D. degree in environmental engineering, working on the development of an innovative system for storing and managing large volumes of satellite data.

Since 2006, she has been collaborating with the Institute of Methodologies for Environmental Analysis, National Research Council, Tito Scalo, Potenza.

Her main interests are the study of methodologies and techniques for the analysis and processing of multitemporal satellite data for environmental research. In particular, she is responsible for the design and development of suitable software for the analysis of a long-term series of high-temporal-resolution satellite data. She is the author of several peer-reviewed scientific journal articles. She has also been a Coinvestigator of several European Union, Italian Space Agency, and CNR projects.



Teodosio Lacava (M'11) was born in Potenza, Italy, in 1972. He received the Master's degree in geological sciences and the Ph.D. degree in methods and technologies for environmental monitoring from the University of Basilicata, Potenza, in 1999 and 2004, respectively.

Since 2005, he has been a Researcher with the Institute of Methodologies for Environmental Analysis, Italian National Research Council (CNR), Tito Scalo, Potenza. His main interests are in the field of satellite data analysis for environmental research,

particularly regarding the development and assessment of advanced satellite techniques for natural hazard investigation. In particular, his work is based on the analysis of high-temporal-resolution satellite data acquired both in the optical and microwave ranges of the electromagnetic spectrum. He has been a Coinvestigator of several European Union, Italian Space Agency, and CNR projects. He is the author of several peer-reviewed scientific journal articles. He also served as a referee for many international journals.

Dr. Lacava is a member of the American Geophysical Union.



Nicola Pergola received the Master's degree in physics from the University of Rome "La Sapienza," Rome, Italy, on May 1993. Since 1998, he has been a Researcher with the Institute of Methodologies for Environmental Analysis (IMAA), National Research Council (CNR), Tito Scalo, Potenza, Italy, where he leads the "Geohazards" Unit of the IMAA Satellite Remote Sensing Laboratory. He was a member of the "core team" Geohazards within the Integrated Global Observing Strategy project, contributing to the definition of new global observational strategies

for geohazard mitigation. He was a Scientific Coordinator for different Italian Space Agency and CNR projects and a Coinvestigator of several European Union and international (e.g., ESA, NATO, and INTAS) projects. He was recently involved in several FP6 and FP7 projects. His main interests are in the field of development of advanced satellite data analysis, particularly regarding high-temporal-resolution sensors like NOAA-AVHRR, EOS-MODIS, and MSG-SEVIRI for environmental research and applications. In particular, his research activity is mainly focused on the development of robust satellite techniques for natural hazard investigation from space and on multitemporal satellite data analysis in the space-time domain, particularly using infrared satellite radiances. He is the author of about 50 papers on ISI journals and more than 150 publications and proceedings with peer reviewing and international distribution. He also serves as a referee for several relevant international journals and is an associate editor of the international scientific journal *Geomatics, Natural Hazards and Risks* (Taylor & Francis Ed).

Dr. Pergola is a member of the European Geosciences Union.



Valerio Tramutoli was born in December 28, 1957. He received the Master's degree in physics from the University of Rome "La Sapienza," Rome, Italy.

Since 1990, he has been with the Department of Engineering and Physics of the Environment (DIFA), University of Basilicata, Potenza, Italy, as a Senior Researcher (since 1993) holding (since 1997) courses of Satellite Remote Sensing at the Faculties of Sciences and Engineering. Since 1991, he has been a Visiting Scientist at the main international centers involved in the Earth's observation by satellite,

taking part in several international projects and initiatives of the main space agencies like ESA, NASA, NASDA, and the Italian Space Agency (ASI). He has been the National Coordinator of the SEISMASS Project (funded by ASI), and the Principal Investigator, or person responsible for DIFA participation, to several international projects funded by NATO and EC in the framework of the Science for Peace, FP6-IST, FP6-INTAS, and FP6+FP7 GMES initiatives. Since 2010, he has been the Coordinator of the European Project PRE-EARTHQUAKES funded by EC in the framework of the FP7-GMES-Space Program. His research activity has been focused on the development of new satellite sensors and techniques for natural, environmental, and technological hazard monitoring and mitigation. In this context, in 1998, he proposed the original RAT (now, RST) change detection approach, which was successfully used in a large spectrum of applications. He has been among the few scientists invited to participate, since 2001, to the IGOS-Geohazard Core Team instructed (by the most important space agencies, CEOS, FAO, UNESCO, ICSU, etc.) to define the new observational strategies for geohazard mitigation for the next decade. He served as Referee for the most important journals in the field and as Project Evaluator for several funding agencies at the European and extra-European levels. Since 2009, he has been a member of the Editorial Board of the international journal *Geomatics, Natural Hazards and Risk*. He is the author or coauthor of more than 150 papers published on international journals, scientific books, and international conference proceedings. He has been the Chair, Cochair, Organizer, or invited Speaker in the most important international conferences (EGU, AGU, and IUGG). Since 2007, he has been a permanent member of the IUGG Inter-Association Working Group on Electromagnetic Studies of Earthquakes and Volcanoes.